Is “Outperform” Still Appropriate to Qualify the Simulation Results of Proposed Protocols for WSNs?

Affoua Thérèse Aby[1,3], Stéphane Pomportes[1,3], Marie-Françoise Servajean[2,4], and Michel Misson[2,4]
[1] ESIEE, Centre de Transfert de Technologie, 14 Quai de la Somme, 80080 Amiens, France
[2] Université Clermont-Auvergne, LIMOS, BP 10448, F-63000 Clermont-Ferrand, France
[3] MIS: Laboratoire Modélisation, Information, Systèmes, Amiens, France
[4] CNRS, UMR 6158, LIMOS, F-63175 Aubière, France
Email: {aby,pomportes}@esiee-amiens.fr; {m-francoise.servajean, michel.misson}@uca.fr

Abstract —Wireless Sensor Networks (WSNs) are the subject of many proposals to improve performance in terms of data delivery ratio, end-to-end delay and energy consumption. To estimate the validity and performance of these proposals, comparisons with the existing protocols are made via simulation tools such as NS2/3, OMNeT++, Glomosim, OPNET, etc. It is interesting to note that in a multitude of scientific articles we can read a variant of: “our proposed protocol outperforms…, ” in the conclusions. This type of conclusion is used even when the simulations only find an increase of a few percent. Although it is not false this statement should be interpreted differently. In this paper we will show, by a comparison of two MAC protocols, and two routing protocols, that the choice of simulation parameters can have a much stronger influence than a gain of a few percent. Thus, we will try to demonstrate that the word ”outperforms” is dependent on the conditions of simulations that are very often only partially specified in the articles. This analytical study allows us to suggest that, it would be more judicious at first to completely detail the simulation environment and to conclude instead of ”our proposed protocol outperforms ...” by ”for the simulation set precisely defined in part xx of this contribution ... ”. In addition, if the simulation conditions are clearly specified, they will be reproducible and make the comparison of results with other protocols easier and more accurate.

Index Terms—WSNs, MAC/Routing protocols, performance evaluation, simulation environment

I. Introduction

WSN is composed of low-cost, energy-independent devices. They can monitor physical or environmental conditions (temperature, humidity, noise, vibration, pressure, motion, pollution, etc.), perform some calculations, and collaborate to transmit their data *via* wireless links to a data collector. This type of network is increasingly used in many emerging applications such as in Industry 4.0 [1], [2], forest fire detection [3], water quality monitoring [4], health [5] and understanding of natural phenomena such as landslides [6], etc. The strong potential of wireless sensor networks is also distinguished by the wealth of literature surrounding research topics about them. The common goal in all these proposals is to find solutions to deal with the limited intrinsic resources of sensor nodes such as: the low range and throughput, the limited amount of energy, the low memory and storage, the reduced computing power.

In most of these works, without having a real production network (which can be very expensive), simulations using tools like NS2/3, OMNeT++, Glomosim, OPNET, etc., are performed to evaluate the performance of proposed protocols. In these performance evaluations, comparisons with other existing protocols are made. It is interesting to note that in a multitude of scientific articles about this research topic, we see conclusions similar to: “our proposed protocol outperforms ...”. This type of conclusion is used even when the simulations give a gain of a few percent. Moreover, in many cases the enhancement of a few percent gain goes far beyond the level of detail on the simulation parameters used to obtain the results. In this paper, we will try to show that the word ”outperform” is very dependent on these simulation conditions (radio frequency, antenna, model propagation, power transmission, capture effect, type of topologies, type of data traffic, etc.) which are often partially specified in the articles. These omissions do not allow the reproducibility of the results obtained and make comparisons more difficult and less relevant.

We previously independently studied in [7], [8], the impact of some simulation parameters on the results obtained with two MAC protocols. In this paper we study the general impact of these parameters with two MAC protocols and two routing protocols. Let’s take the case of works based on the implementation of a mechanism to ensure a long networks life time.

At first, we use two duty cycle MAC protocols. In this type of protocols, nodes sequence periods of activities and inactivities to save energy by disabling the most energy consuming module (the radio module) during the inactivity period. The duty cycle represents the ratio between the active period (during which the radio module is on) and the global period (active period + inactive period). The main MAC protocol based on this principle is the standard IEEE 802.15.4 [9] in beacon-enabled mode, which is one of two tested MAC protocols. In the beacon enabled mode of the standard, the activity and

Manuscript received April 2, 2019; revised September 27, 2019.
Corresponding author email: abytherese@yahoo.fr.
doi:10.12720/jcm.14.11.987-1001

inactivity periods of the nodes are synchronized. Generally, protocols based on this principle are called synchronous duty cycle protocols. Contrary to this mechanism, in the second tested MAC protocol (*SlackMAC* [10], [11]), the nodes do not need to agree for their periods of activity and inactivity. This second category is called asynchronous duty cycle protocols. In a second step, we perform tests with two routing protocols from the literature based on the same MAC mechanism. These protocols have been chosen in such a way that by intuition, we know in both cases that one outperforms the other unambiguously. We do not make an exhaustive comparative study between protocols, in this paper we will try to show the gap in the results according to different sets of parameters of the simulation environment. Papers such as [12]-[15] show for example, the impact of topologies and propagation models on simulation results. In this paper we go further and make a complete and detailed study focusing on several important parameters of the simulation environment.

For the comparison of protocols, we selected some parameters which have a great influence on the results but which are often not clearly specified: the topology, the data generation period, the capture threshold and the propagation model. For this last parameter, we will use the shadowing propagation model and choose more particularly to provide a comparison according to standard deviation and the path loss exponent. This analytical study allows us to suggest that it would be more judicious at first to completely detail the simulation environment and to conclude with “for the simulation set precisely defined in part xx of this contribution…” instead of with “our proposed protocol outperforms...”.

This paper is organized as follows. In section II, we show the role of the main parameters of simulations which are often neglected. In section III, we perform a critical analysis of the simulation environment specification in duty cycle MAC/Routing protocols of the literature. Section IV, presents results by simulations derived from this analysis. Finally in section V, we provide the conclusions of our study.

II. Preliminary Study

This part shows the role of the main simulation parameters, which greatly influence the results but are often not clearly defined in the literature. These main parameters are the topology, the propagation model and the capture effect.

A. Topology Production Strategy

The rules for generating topologies and the importance of their specifications in the simulations have been detailed in [7]. Fig. 1, Fig. 2, Fig. 3 and Fig. 4 are examples of the four types of topologies we will use for the tests in section IV.

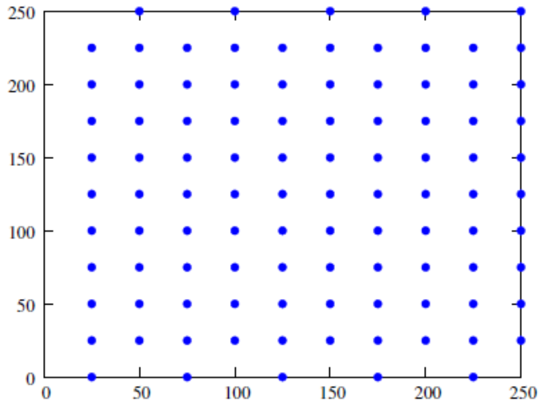

Fig. 1. Topology in square (250 m x 250 m) with 100 nodes positioned in the grid.

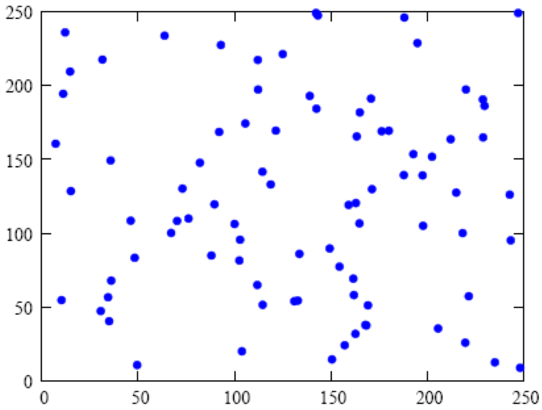

Fig. 2. Topology in square (250 m x 250 m) with 100 nodes randomly positioned.

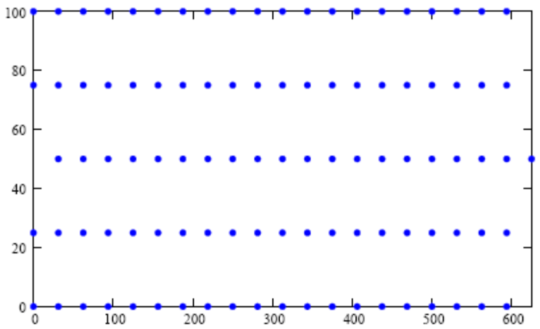

Fig. 3. Pseudo-linear topology (625 m x 100 m) with 100 nodes positioned in the grid.

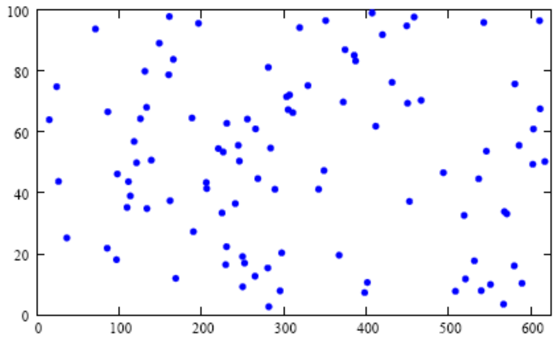

Fig. 4. Pseudo-linear topology (625 m x 100 m) with 100 nodes randomly positioned.

B. Propagation Model

There are several types of propagation models, let's take for example the three main ones which are: Free Space [16], Tow-Ray Ground [17] and Log-normal Shadowing. The free space model is used to represent the reception power of the signal between transmitter and receiver in an ideal case, where the environment is devoid of any obstacle. This representation is done using the Friis formula defined in equation (1).

$$P_r(d) = \frac{P_t G_t G_r \lambda^2}{(4\pi)^2 d^2} \quad (1)$$

The parameters are respectively: Pt: transmission power, G_t: antenna gain of the transmitter, G_r: antenna gain of the receiver, d: distance between transmitter and receiver, λ: signal wavelength. Since the Friis model is not realistic (it does not take into account any obstacle, reflection, refraction, diffraction that the signal can suffer), the Two-Ray Ground reflected Model has been proposed to take into account the reflection of the ground. This model assumes that in terrestrial communication, the signal received by the receiver has two components: the direct signal and the signal coming from the ground reflection (see Fig. 5).

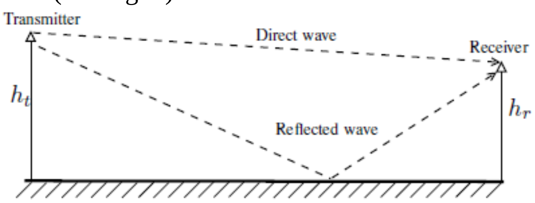

Fig. 5. Two-Ray ground reflection

Equation (2) gives the formula that provides the reception power taking into account the antenna height of the transmitter (h_t) and the receiver (h_r).

$$P_r(d) = \frac{P_t G_t G_r h_t^2 h_r^2}{d^4} \quad (2)$$

The resulting path loss (in equation (3)) is much larger than in Friis model.

$$PL(d)[dB] = \frac{P_t}{P_r} = \frac{d^4}{G_t G_r h_t^2 h_r^2} \quad (3)$$

The Log-normal Shadowing model is based on the semi-empirical Log-distance Path Loss model that is a combination of experimental and theoretical measurement. In Log-distance Path Loss model, the path loss is represented (4):

$$PL(d)[dB] = PL(d_0) + 10\gamma \log \frac{d}{d_0} \quad (4)$$

where PL(d_0) is a theoretical estimation of the path loss for a reference distance d_0 (generally equals to 1m) and γ is the path loss exponent that varies depending on the environment. An estimate of path loss exponent as a function of the environment achieved in [18] is summarized in Table I.

TABLE I: PATH LOSS EXPONENT [18].

Environment		γ
Inside	With direct line of sight	[1.6, 1.8]
	Without direct line of sight	[4, 6]
Outside	Free space	2
	Urban area with diffraction	[2.7, 5]

Log-distance Path Loss does not take into account the variation of the reception power caused by environment effects [19]. The Log-normal Shadowing model adds a correction factor in dB as a random variable to take the variations into account. Thus the formula of the path loss becomes (5):

$$PL(d)[dB] = PL(d_0) + 10\gamma \log \frac{d}{d_0} + X_\sigma \quad (5)$$

where Xσ (Gaussian distribution) represents this corrective factor in dB with σ his standard deviation. Shadowing standard deviation values according to the environment achieved in [17] is given in Table II.

TABLE II. LOG-NORMAL SHADOWING STANDARD DEVIATION [17].

Environment	σ (dB)
Outside	[4, 12]
Factory with direct line of sight	[3, 6]
Factory without direct line of sight	6.8
Building with obstacle	9,6
Building with few obstacle	7

C. Capture Effect

A frame *f* with reception power of P_f is captured when it is received simultaneously with n other frames, and P_f is greater than or equal to the sum of the other reception power and the defined power threshold. This minimum power threshold in dB represents the capture threshold. In figure 6, a frame *f* and other competing frames f_1, f_2, f_3, f_4 are received simultaneously. Let's note: P_f the reception power of frame *f*, the competing frames reception power and *CTx* the capture threshold. Let's note: P_f the reception power of frame *f*, $\sum_{k=1}^{n} P_{fk}$ the competing frames reception power and *CTx* the capture threshold.

- If $P_f \geq \sum_{k=1}^{n} P_{fk} + CTx$, the frame *f* will be captured and will represent a successful reception which will be correctly decoded.

- Otherwise, all these simultaneous receptions will be considered as a collision.

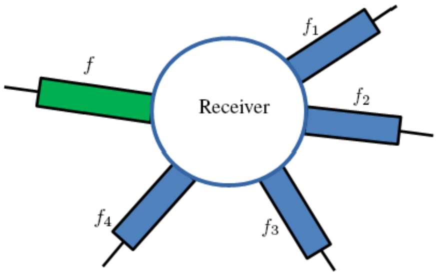

Fig. 6. Capture effect illustration.

Therefore, the value set for the capture threshold has an impact on the collision ratio. Moreover, this impact will be more important in the case where the network traffic is intense.

III. Survey on Simulation Conditions Specification

This part summarizes what the specifications of the parameters described in section II during performance evaluations of MAC and Routing protocols for WSNs in literature are about.

A. MAC Protocols

In the literature, the duty cycle MAC protocols are classified into two main categories such as synchronous duty cycle MAC protocols and asynchronous duty cycle MAC protocols.

The standard IEEE 802.15.4 [9] in beacon enabled mode is one of the main synchronous duty cycle MAC protocols. In this standard, all nodes are synchronized for their period of activity and inactivity. Protocols based on the same principle in which synchronization is global are: protocol in [20] and LO-MAC (Low Overhead MAC) [21]. There are also other synchronization variants in which the nodes synchronize locally according to a tree topology. Protocols like D-MAC (Data-gathering MAC) [22] and TreeMAC [23] are based on this mechanism. ID-MAC (An identity-based MAC) [24], DW-MAC (Demand Wakeup MAC) [25], EDS-MAC (Energy Efficient Dynamic Scheduling Hybrid MAC) [26] and iCore (An incast-collision-free data collection protocol) [27] are improved versions of these type of protocols.

Asynchronous duty cycle MAC protocols do not require synchronization between nodes. Nodes start their activity and inactivity periods independently. These types of protocols are either initiated by the sender, the receiver or both (sender and receiver). The protocol B-MAC (Berkeley MAC) [28] is the main sender-initiated MAC protocol, in which when a node has a packet to send, it starts by sending a long preamble to allow the receiver to detect it and remain active to receive the packet. Improvements of B-MAC are proposed in X-MAC (A short preamble MAC) [29], BoX-MAC [30] and OSX-MAC (On-demand synchronous X-MAC protocol) [31] to reduce the size of the preamble (thus reducing the activity period of the sender).

TABLE III: Survey on the Specification of Simulation Conditions in Duty Cycle MAC Protocols Using NS2 Simulator

Simulation conditions/ Protocols	Radio Frequency	Antenna: -type -gain -height	Propagation model	TX power	Topology: -type -size -TX range -number of nodes -sink position	-RXThresh_ -CSThresh_	Traffic: -type -size -period	Queue size or Buffer	Capture Threshold
DW-MAC [25]	✓	1/3	✓	✓	✓	✗	✓	✗	✗
LO-MAC [21]	✓	1/3	✓	✓	✓	✓	2/3	✗	✗
ID-MAC [24]	✗	✗	✗	✓	✓	✗	2/3	✗	✗
EDS-MAC [26]	✓	✗	✗	✗	✓	✗	✓	✗	✗
iCore [27]	✗	✗	✓	✗	✓	✗	1/3	✗	✗
OSX-MAC [38]	✗	✗	✗	✓	1/5	✓	1/3	✗	✗
OC-MAC [34]	✗	✗	✗	✗	✓	✗	2/3	✗	✗
RIX-MAC [33]	✗	1/3	✓	✓	3/5	✓	✓	✗	✗
[35]	✗	✗	✓	✗	✓	✗	2/3	✗	✗
ERI-MAC [32]	✓	✗	✗	✓	✓	✗	2/3	✗	✗
[36]	✗	✗	✓	✓	✓	✗	2/3	✗	✗
SlackMAC [11], [10]	✗	✗	✓	✓	✓	✗	2/3	✓	✗

Unlike sender-initiated MAC protocols in which the sender initiates the communication, in receiver-initiated MAC protocols, the receiver sends a beacon when it goes into active mode to inform the sender about its ability of receive data. One of the main protocols based on this principle is RI-MAC. Other mechanisms for reducing the receiver load are proposed in ERI-MAC (An Energy-Harvested RI-MAC) [32], RIX-MAC (Receiver-Initiated X-MAC) [33], OC-MAC (Opportunistic Cooperation MAC protocol) [34] and protocol in [35].

Unlike the previous two, in the hybrid MAC protocols, either the sender or the receiver can initiate communication, thus ensuring a fair level of communication load and energy consumption. Protocol in [36] and SlackMAC [10], [11] are based on this principle.

In most of the protocols cited above (as improvements to other protocols), comparisons are done using the NS-2

[37] simulator to show that the proposed protocols outperform existing ones. Table III shows a summary of the simulation conditions specification in these performance evaluations. Most of the time we notice that the simulation environment is only partially described. There are proposals in which the antenna information is not provided, although these parameters are taken into account to calculate the reception power as shown in section II. Sometimes, the topologies used to perform the tests are not clearly defined. The information about the data, which depending on the application (may can be low bit rate or high bit rate with a limited size) and the buffer size that acts on the end-to-end delay, is also not fully provided. It can also be seen that the capture threshold, which is an important parameter in collision management, is not specified in any of the protocols in the Table III.

B. Routing Protocols

Several routing protocols for WSNs are proposed in the literature. Among these protocols, simulation comparisons are made with existing protocols. For this study, we take the simulation conditions of some routing protocols based on a MAC duty cycle mechanism as an example. These types of protocols are commonly called opportunistic routing protocols. We mainly distinguish between opportunistic gradient-based and flooding-based routing protocols.

In opportunistic gradient-based routing protocols, a metric commonly called a gradient is computed according to parameters such as, distance or number of hops, residual energy, reliability of links, etc. It is on the basis of this metric that data is routed hop by hop from source nodes (next relay is one of nodes with a lower metric) to the sink. Protocols like DSRSS (Dijkstra's shortest path routing and sleep-wake scheduling) [39], OVAR (An opportunistic void avoidance routing protocol) [40], OAODV (Opportunistic AODV routing protocol) [41], EFFORT (Energy-efficient opportunistic routing technology) [42], literature, the duty cycle MAC protocols are classified into two main categories such as synchronous duty cycle MAC protocols and asynchronous duty cycle MAC protocols.

Table IV gives a summary of the description of simulation conditions performed, in performance evaluation on NS2 [37], to show that the proposed protocols outperform the existing. As in the MAC protocols previously shown, the description of the simulation environment is often not fully defined and sometimes non-existent.

TABLE IV: SURVEY ON THE SPECIFICATION OF SIMULATION CONDITIONS IN OPPORTUNISTIC ROUTING PROTOCOLS USING NS2 SIMULATOR

Simulation conditions/ Protocols	Radio Frequency	Antenna: -type -gain -height	Propagation model	TX power	Topology: -type -size -TX range -number of nodes -sink position	-RXThresh_ -CSThresh_	Traffic: -type -size -period	Queue size or Buffer	Capture Threshold
OVAR [40]	×	×	√	√	√	×	2/3	×	×
DSRSS [39]	×	×	×	×	√	×	√	×	×
ETOR [43]	×	×	√	×	√	×	√	√	×
OAODV [41]	×	1/3	√	×	3/5	×	2/3	√	×
EFFORT [42]	×	×	×	√	√	×	2/3	×	×
ASSORT [44]	√	×	×	×	√	×	√	×	×
CF [51]	√	×	×	×	4/5	×	√	×	×
EADCR [50]	√	×	√	√	√	×	2/3	√	×
LEOA [47]	√	×	√	×	√	×	×	×	×
MDET [45]	√	√	√	×	√	×	√	×	×
DSRF [48]	√	√	√	√	√	√	2/3	√	×
DEF [49]	√	×	√	×	√	×	×	×	×

Likewise, this study allowed us to realize that, in addition to the simulation environment (which is not described as it should be), there are a lot of papers in which the platform used to perform the simulations is not mentioned anywhere. Protocols like [52]-[61], etc., are examples of opportunistic routing protocols in this case.

In the following section, we perform an intensive simulation to show the gap in the results according to different sets of parameters of the simulation environment.

IV. VERIFICATION BY SIMULATION

In this section we have carried out intensive simulations to show the gap in the results according to simulation parameters using two MAC protocols (SlackMAC [10], [11] and the standard IEEE [9]) and two opportunistic flooding-based routing protocols (E-ADCR [50] and CF [46]).

We begin by describing the parameters used for the simulation and then the results in four different scenarios.

A. Simulation Environment

We performed simulations with the NS-2 [37] simulator. Table V describes the global parameters of the simulation.

The types of topologies used are like those described in section II (see figures 1, 2, 3 and 4). Each topology has 100 nodes positioned in grid or randomly on a square or pseudo-linear area. We use 10 topologies per type defined in the figures and carry out 10 repetitions of the simulations.

TABLE V: GLOBAL SPECIFICATION OF THE SIMULATION ENVIRONMENT.

Parameters	Values
Total number of nodes	100
Number of source nodes	30
Topologies area	Square: 250mx250m and Pseudo-linear: 625mx100m
Transmission range	50 m
Radio frequency	2.4 GHz
RXThresh (Receive threshold)	-85 dBm
CSThresh (Carrier-sense threshold)	-92 dBm
Capture threshold	[2dB, 10dB]
System loss (L)	1
Antenna type	Omnidirectional
Antenna gain (Gt, Gr)	1
Antenna height (Z)	1.5 m
Propagation model: Log-normal Shadowing	Path loss exponent: [2, 3]
	Standard deviation: [2dB, 8dB]
Data traffic type	CBR (Constant-bit rate)
Packet size	30 bytes
Data generation period	[5 seconds, 60 seconds]
Buffer size	20 frames
Number of topology per type	10
Repetitions per topology	10
Simulation duration	1 hour

The convergecast communication is used: 30 source nodes randomly located in the network perform measurements periodically and route them hop by hop to the sink (located in the upper right corner of the area). In the evaluation of MAC protocols a gradient-based routing protocol is used to route packets from the source nodes to the sink. Nodes have an active period of 50 ms every 5 s, which corresponds to a duty cycle of 1%. Remember that the two routing protocols are based on a duty cycle MAC mechanism. Each point on the following curves is an average of the simulation of 10 times each of the 10 topologies. The outage probability method specified in [62], [63] and summarized in [8] is used to determine the transmission power. This method provides a stability of the radio links ensuring 95% reception ratio between two nodes. Table VI gives the associated transmission power to be used based on the propagation model parameters specified in Table V (*eg*. shadowing Path Loss between 2 and 3, standard deviation between 2dB and 8dB) and the transmission range of 50m.

TABLE VI: ASSOCIATED TRANSMISSION POWER (PT) IN DBM USING OUTAGE PROBABILITY METHOD

Path L. E. / Std. D. (dB)	2.0	2.5	3.0
2	-1,240	7,254	15,749
4	2,039	10,534	19,029
6	5,319	13,814	22,309
8	8,599	17,094	25,589

The two test MAC protocols: the standard IEEE 802.15.4 [9] and SlackMAC [11], [10]) and the two test routing protocols: E-ADCR [50] and CF [46]) are evaluated in four different scenarios.

The objective is to evaluate the impact of different simulation parameters respectively. We evaluate the impact of shadowing path loss exponent in scenario 1, the impact of shadowing standard deviation in scenario 2, the impact of data generation period in scenario 3 and finally in scenario 4 the impact of the capture threshold. In each of these scenarios, a test with different types of topologies is performed. We note: **SquLat** to represent topologies in square with grid positioning and **SquRnd** for square topologies with random positioning. In the same way we represent pseudo-linear topologies with respectively in grid and at random positioning by **StrLat** and **StrRnd**.

The metrics evaluated are the delivery ratio and the average end-to-end delay for data packets. The data packets delivery ratio (denoted TL) represents the ratio between the number of data packets received by the sink (denoted PR) divided by the total number of packets generated (denoted PG) by source nodes in the network:

$$TL = \frac{PR}{PG} * 100 .$$

The average delay (or latency) of packets delivered represents the average time taken for data packets to get from the source nodes to the sink. The main causes of data packet delay are: the propagation delay (very low), the transmission delay, the processing time and the time spent in the queue. Here, we compute this delay (denoted d_{pi} for delay of packet *i*) by making the difference between the packet reception date (denoted D_r) by the sink and the initial generation date of this packet (denoted D_i): $d_{pi} = D_r - D_i$. Thereafter, the average end-to-end delay (d_m) for n received packets is:

$$d_m = \frac{\sum_{i=1}^{n} (d_{pi})}{n}$$

B. Simulation Results

1) Scenario 1: impact of shadowing path loss exponent

In this scenario, the shadowing standard deviation is set to 4dB, the capture threshold is 5dB and the data generation period is 30 seconds. In each case of topology area (square and pseudo-linear), we vary the shadowing path loss exponent value between 2 and 3.

Results of MAC protocols

Fig. 7 and Fig. 8 respectively show data delivery ratio and average delay for both MAC protocols (the standard and SlackMAC), according to the shadowing path loss exponent (between 2 and 3), with a topology area in square and pseudo-linear, when in each case nodes are positioned in grid and randomly.

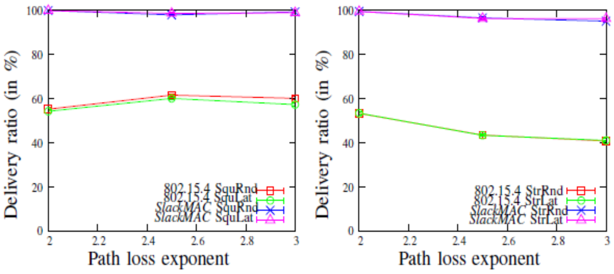

Fig. 7. Data delivery ratio for both MAC protocols: the standard and SlackMAC, according to the shadowing path loss exponent, with the results for a square topology on the left and those for a pseudo-linear topology on the right.

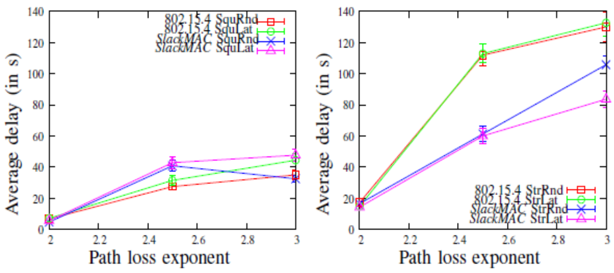

Fig. 8. Average data delivery delay for both MAC protocols: the standard and SlackMAC, according to the shadowing path loss exponent, with the results for a square topology on the left and those for a pseudo-linear topology on the right.

For the standard IEEE 802.15.4:

- In the case of square topologies, the data delivery ratio balances between 54.26% and 61.58% with a variation of the path loss exponent from 2 to 3. However, there is a slight increase for a random positioning of the nodes (between 55.19% and 61.58%) compared to a grid positioning (between 54.26% and 60.1%). The same behavior is remarked at the average delay level, which is slightly lower when the nodes are random positioning (increases from 6.85 s to 35.3 s) compared to the grid positioning (increases from 7.3 s to 44.47 s) when the path loss exponent increases from 2 to 3.

- In the case of pseudo-linear topologies, the delivery ratio decreases from 53.41% to 40.77% with a variation of the path loss exponent (between 2 and 3) and remains almost the same for both types of nodes positioning (random and grid). The average delay increases when the path loss exponent increases for both types of nodes positioning (from 14.94 s to 132.56 s for grid positioning and from 17.33 s to 129.92 s for random positioning).

For SlackMAC:

- In the case of square topologies, the data delivery ratio balances between 98.04% and 99.98% with a variation of the path loss exponent (between 2 and 3). However, there is a slight increase for a random positioning (between 98.73% and 99.98%) compared to a grid positioning of the nodes (between 98.04% and 99.98%). The average delay also balances when the path loss exponent increases from 2 to 3, for both types of nodes positioning (between 4.81 s and 40.89 s for random positioning and between 5.7 s and 47.69 s for grid positioning).

- In the case of pseudo-linear topologies, the delivery ratio decreases from 99.58% to 95.20% with a variation of the path loss exponent (between 2 and 3) and remains almost the same for both types of nodes positioning (random and grid). The average delay increases when the path loss exponent increases for both types of nodes positioning (from 17.33 s to 129.92 s for random positioning and from 14.94 s to 132.56 s for grid positioning).

Results of routing protocols

Fig. 9 and Fig. 10 respectively show data delivery ratio and average delay for both routing protocols (CF and E-ADCR), according to the shadowing path loss exponent (between 2 and 3), with a topology area in square and pseudo-linear, when in each case nodes are positioned in grid and randomly.

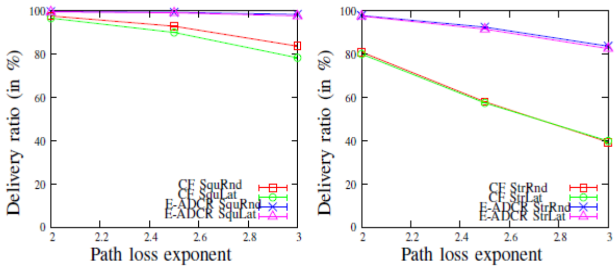

Fig. 9. Data delivery ratio for both routing protocols: CF and E-ADCR, according to the shadowing path loss exponent, with the results for a square topology on the left and those for a pseudo-linear topology on the right.

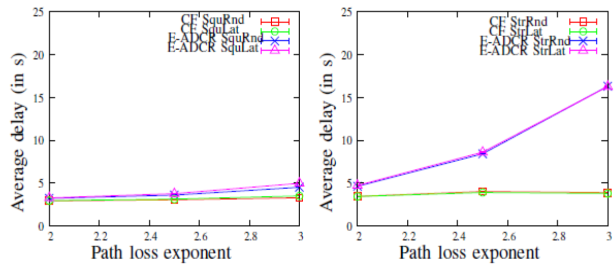

Fig. 10. Average data delivery delay for both routing protocols: CF and E-ADCR, according to the shadowing path loss exponent, with the results for a square topology on the left and those for a pseudo-linear topology on the right.

For CF:

- In the case of square topologies, the delivery ratio decreases for both types of nodes positioning, with a slight increase for a random positioning (from 97.69% to 80.70%) compared to a grid positioning (from 96.66% to 78.30%) when the path loss exponent increases from 2 to 3. The average delay slightly increases (from 2.94 s to 3.3 s for random positioning and from 2.96 s to 3.51 s for grid positioning) with the path loss exponent.

- In the case of pseudo-linear topologies, the delivery ratio decreases from 80.98% to 39.31% with a variation of the path loss exponent (between 2 and 3) and remains almost the same for both types of nodes positioning (grid and random). The average delay balances between 3.46 s and 4.03 s for random positioning and between 3.45 s and3.91 s for grid positioning, when the path loss exponent increase from 2 to 3. For E-ADCR:

- In the case of square topologies, the delivery ratio decreases slowly when the path loss exponent increases unlike CF, for both types of nodes positioning (from 99.71% to 98.40% for random positioning and from 99.62% to 97.73% for grid positioning). As in CF protocol, the average delay slightly increases (from 3.23 s to 4.52 s for random positioning and from 3.30 s to 4.98 s for grid positioning) with the path loss exponent.

- In the case of pseudo-linear topologies, the delivery ratio decreases when the path loss exponent increases for both types of nodes positioning (from 97.90% to 83.71% for random positioning and from 97.61% to 82.59% for grid positioning). The average delay also increases when the path loss exponent increases for both types of nodes positioning (from 4.62 s to 16.51 s for random positioning and from 4.73 s to 16.26 s for grid positioning).

In this first scenario, the results show a drop in performance (delivery ratio decreases and average delay increases) according to the shadowing path loss exponent (between 2 and 3), for the two MAC protocols as for the two routing protocols regardless of node position and topologies area. This decrease in performance is explained by the fact that the nodes have fewer neighbors (less meshed network) when the path loss exponent increases. The data will travel more hops (therefore more possibilities of lost packets and the end-to-end delay becomes significant), before reaching the sink.

2) Scenario 2: impact of the shadowing standard deviation

In this second scenario, the value of the shadowing path loss exponent is set to 2.5, the data generation period is 30 seconds and the capture threshold is 5dB. In each case of topology area (square and pseudo-linear), we vary the shadowing standard deviation between 2 dB and 8 dB.

Results of MAC protocols

Fig. 11 and Fig. 12 respectively show data delivery ratio and average delay for both MAC protocols (the standard and SlackMAC), according to the shadowing standard deviation (between 2 dB and 8 dB), with a topology area in square and pseudo-linear, when in each case nodes are positioned in grid and randomly.

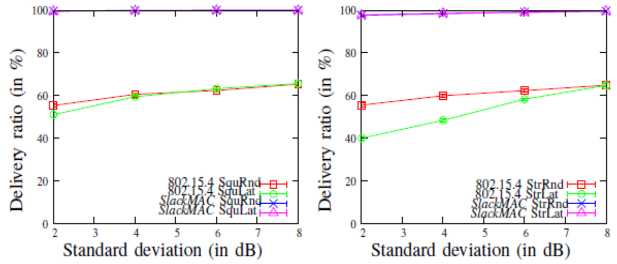

Fig. 11. Data delivery ratio for both routing protocols: CF and E-ADCR, according to the shadowing standard deviation, with the results for a square topology on the left and those for a pseudo-linear topology on the right.

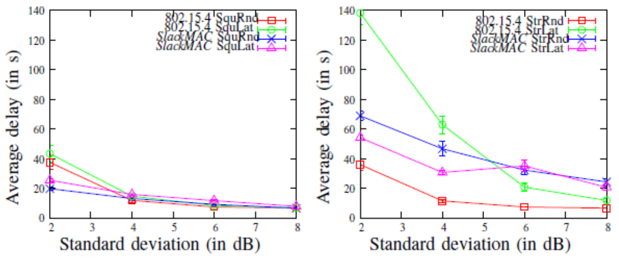

Fig. 12. Average data delivery delay for both MAC protocols: the standard and SlackMAC, according to the shadowing standard deviation, with the results for a square topology on the left and those for a pseudo-linear topology on the right

For the standard IEEE 802.15.4:

- In the case of square topologies, the delivery ratio increases for both types of nodes positioning (from 55.26% to 65.29% for a random positioning of the nodes and from 51.03% to 65.58% for a grid positioning) with the shadowing standard deviation (between 2 dB and 8 dB). The average delay decreases for both types of nodes positioning (from 37.46 s to 6.65 s for a random positioning of the nodes and from 43.40 s to 6.95 s for a grid positioning) when the shadowing standard deviation increases from 2 dB to 8 dB.

- In the case of pseudo-linear topologies, as in square topology, the delivery ratio increases, from 55.44% to 64.80% for a random positioning of the nodes and from 39.96% to 64.70% for a grid positioning with the shadowing standard deviation (between 2 dB and 8 dB). The average delay decreases from 35.97 s to 6.58 s for a random positioning of the nodes and from 138.33 s to 11.78 s for a grid positioning, when the shadowing standard deviation increases from 2 dB to 8 dB.

For SlackMAC:

- In the case of square topologies, the delivery ratio slightly increases for both types of nodes positioning (from 99.64% to 99.98% for a random positioning of the nodes and from 99.53% to 99.98% for a grid positioning) with the shadowing standard deviation (between 2 dB and 8 dB). The average delay decreases for both types of nodes positioning (from 19.72 s to 6.55 s for a random positioning of the nodes and from 24.44 s to 7.83 s for a grid positioning) when the shadowing standard deviation increases from 2 dB to 8 dB.

- In the case of pseudo-linear topologies, the delivery ratio increases (from 97.65% to 99.56% for a random positioning of the nodes and from 97.83% to 99.70% for a grid positioning) with the shadowing standard deviation (between 2 dB and 8 dB). The average delay decreases from 68.91 s to 24.27 s for a random positioning of the nodes and balances between 20.62 s and 54.17 s for a grid positioning, when the shadowing standard deviation increases from 2 dB to 8 dB.

Results of routing protocols

Fig. 13 and Fig. 14 respectively show data delivery ratio and average delay for both routing protocols (CF and E-ADCR), according to the shadowing standard deviation (between 2 dB and 8 dB), with a topology area in square and pseudo-linear, when in each case nodes are positioned in grid and randomly.

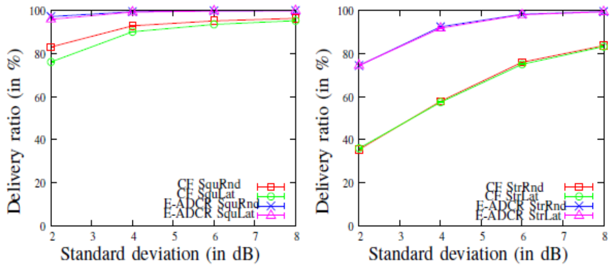

Fig. 13. Data delivery ratio for both routing protocols: CF and E-ADCR, according to the shadowing standard deviation, with the results for a square topology on the left and those for a pseudo-linear topology on the right.

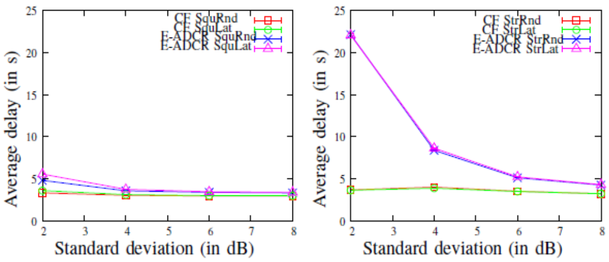

Fig. 14. Average data delivery delay for both routing protocols: CF and E-ADCR, according to the shadowing standard deviation, with the results for a square topology on the left and those for a pseudo-linear topology on the right.

For CF:

- In the case of square topologies, the delivery ratio increases for both types of nodes positioning (from 83.01% to 96.26% for a random positioning of the nodes and from 76.06% to 95.18% for a grid positioning) with the shadowing standard deviation (between 2 dB and 8 dB). The average delay slightly decreases for both types of nodes positioning (from 3.35 s to 2.98 s for a random positioning of the nodes and from 3.63 s to 3.02 s for a grid positioning) when the shadowing standard deviation increases from 2 dB to 8 dB.

-In the case of pseudo-linear topologies, as in square topology the delivery ratio increases (from 35.48% to 83.60% for a random positioning of the nodes and from 36.05% to 83.18% for a grid positioning) with the shadowing standard deviation (between 2 dB and 8 dB). The average delay balances for both types of nodes positioning between 3.25 s and 4.03 s for a random positioning of the nodes and between 3.25 s and 3.90 s for a grid positioning, when the shadowing standard deviation increases from 2 dB to 8 dB.

For E-ADCR:

- In the case of square topologies, the delivery ratio increases for both types of nodes positioning (from 97.07% to 99.85% for a random positioning of the nodes and from 95.82% to 99.83% for a grid positioning) with the shadowing standard deviation (between 2 dB and 8 dB). The average delay decreases for both types of nodes positioning (from 4.84 s to 3.36 s for a random positioning of the nodes and from 5.58 s to 3.42 s for a grid positioning) when the shadowing standard deviation increases from 2 dB to 8 dB.

- In the case of pseudo-linear topologies, unlike in square topology, there is an important increase for the delivery ratio and also an important decrease for the average delay. The delivery ratio increases, from 74.38% to 99.39% for a random positioning of the nodes and from 74.49% to 99.31% for a grid positioning with the shadowing standard deviation (between 2 dB and 8 dB). The average delay decreases from 22.11 s to 4.29 s for a random positioning of the nodes and from 22.06 s to 4.34 s for a grid positioning, when the shadowing standard deviation increases from 2 dB to 8 dB.

In this second scenario, we observe an increase in performance (delivery ratio increase and decrease in average delay) with the shadowing standard deviation for all protocols. It is very low for SlackMAC and E-ADCR, and a little more substantial for the standard and CF. For the standard and CF, this performance increase starts lower for grid positioning than for random positioning. Moreover, for both MAC and routing protocols, the increase in performance remains slightly higher when the zone is square compared to the pseudo-linear zone. Unlike the previous scenario where the increase of the path loss exponent reduced the number of links (nodes in range), when the value of the standard deviation increases, fugitive links are created between nodes, making the network more meshed. This reduces the number of hops for the data to reach the sink and improves performance.

3) Scenario 3: Impact of the data generation period

In this scenario, the value of the shadowing path loss exponent is set to 2.5, the shadowing standard deviation is 4dB and the capture threshold is 5dB. In each case of topology area (square and pseudo-linear), we vary the data generation period between 5 seconds and 60 seconds.

Results of MAC protocols

Fig. 15 and Fig. 16 respectively show data delivery ratio and average delay for both MAC protocols (the standard and SlackMAC), according to the data generation period (between 5 s and 60 s), with a topology area in square and pseudo-linear, when in each case nodes are positioned in grid and randomly.

For the standard IEEE 802.15.4:

- In the case of square topologies, the delivery ratio increases for both types of nodes positioning (from 21.24% to 60.49% for a random positioning of the nodes and from 19.82% to 60.25% for a grid positioning) with the data generation period (between 5 s and 60 s). The average delay hugely decreases for both types of nodes positioning (from 151.25 s to 9.27 s for a random positioning of the nodes and from 153.98 s to 10.21 s for a grid positioning) when the data generation period increases from 5 s to 60 s.

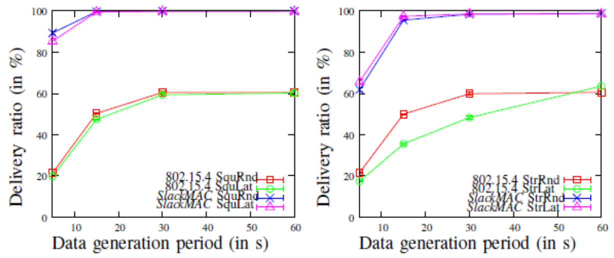

Fig. 15. Data delivery ratio for both MAC protocols: the standard and SlackMAC, according to the data generation period, with the results for a square topology on the left and those for a pseudo-linear topology on the right.

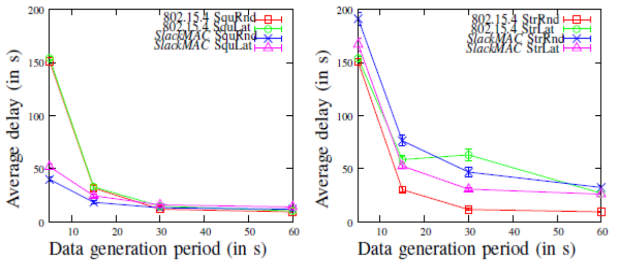

Fig. 16. Average data delivery delay for both MAC protocols: the standard and SlackMAC, according to the data generation period, with the results for a square topology on the left and those for a pseudo-linear topology on the right.

- In the case of pseudo-linear topologies, as in square topology, the delivery ratio increases (from 21.64% to 60.60% for a random positioning of the nodes and from 17.42% to 63.55% for a grid positioning) with the data generation period (between 5 s and 60 s). The average delay hugely decreases from 150.51 s to 9.27 s for a random positioning of the nodes and from 153.86 s to 26.84 s for a grid positioning, when the data generation period increases from 5 s to 60 s.

For SlackMAC:

- In the case of square topologies, the delivery ratio increases for both types of nodes positioning (from 89.33% to 99.93% for a random positioning of the nodes and from 85.35% to 99.91% for a grid positioning) with the data generation period (between 5 s and 60 s). The average delay decreases for both types of nodes positioning (from 39.90 s to 11.77 s for a random positioning of the nodes and from 51.81 s to 13.87 s for a grid positioning) when the data generation period increases from 5 s to 60 s.

- In the case of pseudo-linear topologies, the delivery ratio increases (from 61.88% to 98.85% for a random positioning of the nodes and from 65.64% to 98.66% for a grid positioning) with the data generation period (between 5 s and 60 s). The average delay decreases from 191.23 s to 32.27 s for a random positioning of the nodes and from 166.98 s to 25.95 s for a grid positioning, when the data generation period increases from 5 s to 60 s.

Results of routing protocols

Fig. 17 and Fig. 18 respectively show data delivery ratio and average delay for both routing protocols (CF and E-ADCR), according to the data generation period (between 5 s and 60 s), with a topology area in square and pseudo-linear, when in each case nodes are positioned in grid and randomly.

For CF:

- In the case of square topologies, the delivery ratio increases for both types of nodes positioning (from 90.05% to 92.88% for a random positioning of the nodes and from 85.78% to 89.98% for a grid positioning) with the data generation period (between 5 s and 60 s). The average delay very slightly increases for both types of nodes positioning (from 2.99 s to 3.07 s for a random positioning of the nodes and from 3.04 s to 3.17 s for a grid positioning) with the data generation period (between 5 s and 60 s).

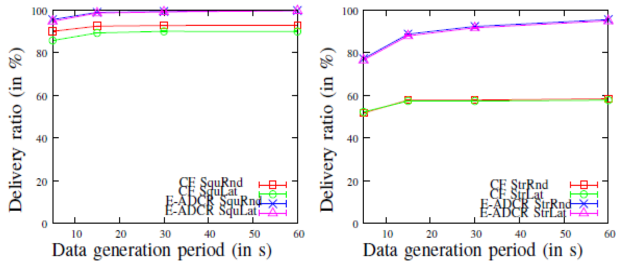

Fig. 17. Data delivery ratio for both routing protocols: CF and E-ADCR, according to the data generation period, with the results for a square topology on the left and those for a pseudo-linear topology on the right.

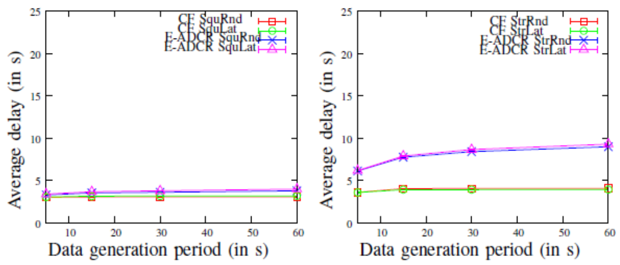

Fig. 18. Average data delivery delay for both routing protocols: CF and E-ADCR, according to the data generation period, with the results for a square topology on the left and those for a pseudo-linear topology on the right.

- In the case of pseudo-linear topologies, as in square topology, the delivery ratio increases (from 51.79% to 58.44% for a random positioning of the nodes and from 52.29% to 57.81% for a grid positioning) with the data generation period (between 5 s and 60 s). The average delay very slightly increases (from 3.59 s to 4.06 s for a random positioning of the nodes and from 3.57 s to 3.92 s for a grid positioning) with the data generation period (between 5 s and 60 s).

For E-ADCR:

- In the case of square topologies, the delivery ratio increases for both types of nodes positioning (from 95.54% to 99.79% for a random positioning of the nodes and from 94.74% to 99.72% for a grid positioning) with the data generation period (between 5 s and 60 s). The average delay very slightly increases (from 3.28 s to 3.77 s for a random positioning of the nodes and from 3.38 s to 3.97 s for a grid positioning) with the data generation period (between 5 s and 60 s).

- In the case of pseudo-linear topologies, as in square topology, the delivery ratio increases (from 77.28% to 95.52% for a random positioning of the nodes and from 76.63% to 94.96% for a grid positioning) with the data generation period (between 5 s and 60 s). The average delay increases (from 6.11 s to 8.97 s for a random positioning of the nodes and from 6.18 s to 9.29 s for a grid positioning) with the data generation period (between 5 s and 60 s).

The results of this scenario show that, there is an increase in performance for all protocols when the data generation period increases. This is explained by the fact that, the network load becomes larger for the low data generation periods and the low duty cycle (1%) does not allow sufficient activity time to route all traffic to the sink. As in scenario 2, for the standard and CF, the performance increase starts lower for grid positioning than for random positioning and for both MAC and routing protocols, the increase in performance remains slightly higher when the zone is square compared to the pseudo-linear zone.

4) Scenario 4: impact of the capture threshold

In this last scenario, the value of the shadowing path loss exponent is set to 2.5, the shadowing standard deviation is 4dB and the data generation period is 30 seconds. In each case of topology area (square and pseudo-linear), we vary the capture threshold between 2 dB and 10 dB.

Results of MAC protocols

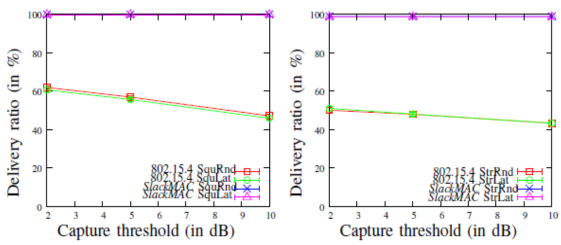

Fig. 19. Data delivery ratio for both MAC protocols: the standard and SlackMAC, according to the capture threshold, with the results for a square topology on the left and those for a pseudo-linear topology on the right.

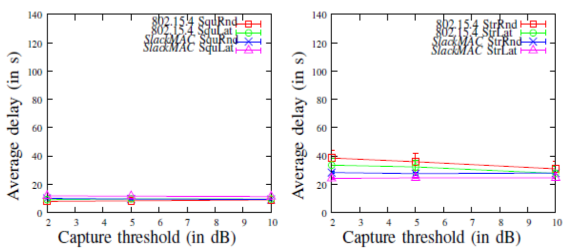

Fig. 20. Average data delivery delay for both MAC protocols: the standard and SlackMAC, according to the capture threshold, with the results for a square topology on the left and those for a pseudo-linear topology on the right.

Fig. 19 and Fig. 20 respectively show data delivery ratio and average delay for both MAC protocols (the standard and SlackMAC), according to the capture threshold (between 2 dB and 10 dB), with a topology area in square and pseudo-linear, when in each case nodes are positioned in grid and randomly.

For the standard IEEE 802.15.4:

- In the case of square topologies, the delivery ratio decreases for both types of nodes positioning (from 61.97% to 47.18% for a random positioning of the nodes and from 60.67% to 45.94% for a grid positioning) when the capture threshold increases from 2 dB to 10 dB. The average delay slightly increases from 7.81 s to 8.86 s for a random positioning of the nodes and remains around 9 s for a grid positioning, when the capture threshold increases from 2 dB to 10 dB.

- In the case of pseudo-linear topologies, as in square topology, the delivery ratio decreases from 50.94% to 43.38% for a random positioning of the nodes and from 51.04% to 43.36% for a grid positioning when the capture threshold increases from 2 dB to 10 dB. The average delay decreases from 38.48 s to 30.84 s for a random positioning of the nodes and from 33.39 s to 27.59 s for a grid positioning, when the capture threshold increases from 2 dB to 10 dB.

For SlackMAC:

- In the case of square topologies, the delivery ratio remains around 99.95% for a random positioning of the nodes and around 99.92% for a grid positioning) when the capture threshold increases from 2 dB to 10 dB. The average delay slightly decreases from 9.91 s to 9.11 s for a random positioning of the nodes and from 11.70 s to 11.22 s for a grid positioning, when the capture threshold increases from 2 dB to 10 dB.

- In the case of pseudo-linear topologies, the delivery ratio remains around 99% for a random positioning of the nodes and around 98.80% for a grid positioning when the capture threshold increases from 2 dB to 10 dB. The average delay remains around 28 s for a random positioning of the nodes and around 24 s for a grid positioning, when the capture threshold increases from 2 dB to 10 dB.

Results of routing protocols

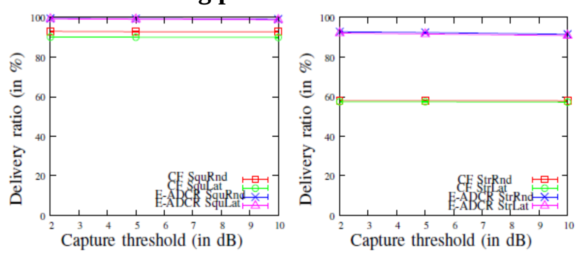

Fig. 21. Data delivery ratio for both routing protocols: CF and E-ADCR, according to the capture threshold, with the results for a square topology on the left and those for a pseudo-linear topology on the right.

Fig. 21 and Fig. 22 respectively show data delivery ratio and average delay for both routing protocols (CF and E-ADCR), according to the capture threshold (between 2 dB and 10 dB), with a topology area in square and pseudo-linear, when in each case nodes are positioned in grid and randomly.

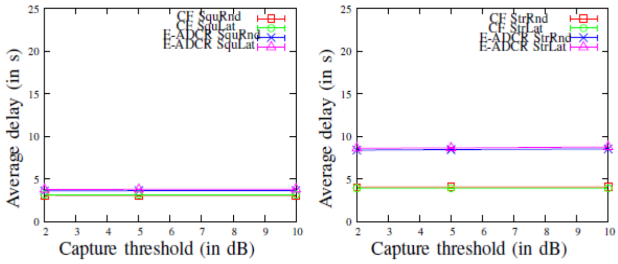

Fig. 22. Average data delivery delay for both routing protocols: CF and E-ADCR, according to the capture threshold, with the results for a square topology on the left and those for a pseudo-linear topology on the right.

For CF:

- In the case of square topologies, the delivery ratio decreases very slightly for both types of nodes positioning (from 92.97% to 92.77% for a random positioning of the nodes and from 90.11% to 89.96% for a grid positioning) when the capture threshold increases from 2 dB to 10 dB. The average delay remains around 3 s for a random positioning of the nodes and around 3.15 s for a grid positioning, when the capture threshold increases from 2 dB to 10 dB.

- In the case of pseudo-linear topologies, as in square topology, the delivery ratio decreases very slightly for both types of nodes positioning (from 58.01% to 57.90% for a random positioning of the nodes and from 57.46% to 57.27% for a grid positioning) when the capture threshold increases from 2 dB to 10 dB. The average delay remains around 4 s for a random positioning of the nodes and around 3.9 s for a grid positioning, when the capture threshold increases from 2 dB to 10 dB.

For E-ADCR:

- In the case of square topologies, the delivery ratio decreases very slightly from 99.49% to 99.13% for a random positioning of the nodes and decreases from 99.32% to 98.87% for a grid positioning, when the capture threshold increases from 2 dB to 10 dB. The average delay remains around 3.6 s for a random positioning of the nodes and around 3.8 s for a grid positioning, when the capture threshold increases from 2 dB to 10 dB.

- In the case of pseudo-linear topologies, the delivery ratio decreases from 92.75% to 91.51% for a random positioning of the nodes and decreases from 92.13% to 90.90% for a grid positioning, when the capture threshold increases from 2 dB to 10 dB. The average delay increases very slightly from 8.37 s to 8.51 s for a random positioning of the nodes and from 8.59 s to 8.73 s for a grid positioning, when the capture threshold increases from 2 dB to 10 dB.

The results of this last scenario show a slight variation of the average delay according to the capture threshold for all protocols. The delivery ratio varies very slightly for SlackMAC and CF, but decreases with a difference of about 14.80 for the standard and 1.25 for E-ADCR when the capture threshold increases. For the standard, since the nodes are synchronized, the number of nodes competing during the activity period is important. Thus, the high collision rate produced for a high capture threshold, explains the best performance in terms of delivery ratio when the capture threshold is low. The drop in performance in terms of the delivery ratio is almost 15% when the capture threshold increases from 2dB to 10dB. However, this parameter is almost never specified in the protocols of the literature for WSNs, performing performance tests by simulation on NS-2.

V. Conclusions

In this work, we made an analytical study on what is really the simulation results of proposed protocols for WSNs that outperform those of the existing. We started by showing the role of the main simulation parameters, then made a state of the art about the description of these parameters when protocols are proposed. Thereafter, we used two MAC protocols and two routing protocols (which we intuitively know that one in both cases outperforms the other unambiguously) to perform intensive simulations. We performed four scenarios in which we evaluated the impact of the parameters (*eg*. the shadowing PathLoss and standard deviation, the data generation period and the capture threshold). In each scenario, we used two topology areas (square and pseudo-linear) with two different positioning of the nodes (random and grid). The results show a significant difference in performance based on a simple set of parameters. For example, for the two tests routing protocols in the case of a square topology with grid positioning and set the value of the shadowing pathLoss to 3, the standard deviation to 4 dB, the capture threshold to 5 dBm and the data generation period to 30 seconds. It can be concluded that, the results of E-ADCR (data delivery ratio is 97.73% and the average delay is 4.98 seconds) ”outperfoms” those of CF (the data delivery ratio is 78.30% and the average delay is 3.51 seconds). However, in the case of square topology with a random positioning, and a set of value of the shadowing pathLoss of 2, a standard deviation of 4 dB, a capture threshold of 5 dBm and a data generation period of 30 seconds. This expression ”outperforms” is not adapted to qualify the results of E-ADCR (the data delivery ratio is 99.71% and the average delay is 3.21 seconds) compared to those of CF (the data delivery ratio is 97.69% and the average delay is 2.94 seconds). However, the literature study shows that very often in the works comparing proposed protocols to those of the existing:

- Simulation environment is partially described or sometimes non-existent
- The difference between the performances is not necessarily important compared to what we showed in this study.

These remarkable differences in performance when simulation conditions change, confirm that: it is very important to clearly define the simulation environment when two protocols are compared, and specify the field of application justifying the choice of retained values. This will contribute to reproducible results and comparisons with other protocols easier and more accurate. Thereby, it would be more suitable to conclude with “for the simulation set precisely defined in part xx of this contribution...” instead of with “our proposed protocol outperforms...”.

REFERENCES

[1] H. H. Khalili, P. R. Green, D. George, G. Watson, and W. Schiffers, “Wireless sensor networks for monitoring gas turbine engines during development,” in *Proc. IEEE Symposium on Computers and Communications*, 2017, pp. 1325–1331.

[2] L. Hou and N. W. Bergmann, “Novel industrial wireless sensor networks for machine condition monitoring and fault diagnosis,” *IEEE Transactions on Instrumentation and Measurement*, vol. 61, no. 10, pp. 2787–2798, 2012.

[3] D. A. R. Valente and P. Vieira, “Forest fire finder–doas application to long-range forest fire detection,” *Atmospheric Measurement Techniques*, vol. 10, no. 6, pp. 2299–2311, 2017.

[4] B. O’Flyrm, R. Martinez, J. Cleary, C. Slater, F. Regan, D. Diamond, and H. Murphy, “Smartcoast: a wireless sensor network for water quality monitoring,” in *Proc. 32nd IEEE Conference on Local Computer Networks*, 2007, pp. 815–816.

[5] S. Kim, S. Pakzad, D. Culler, J. Demmel, G. Fenves, S. Glaser, and M. Turon, “Health monitoring of civil infrastructures using wireless sensor networks,” in *Proc. 6th International Conference on Information Processing in Sensor Networks*, 2007, pp. 254–263.

[6] G. R. Teja, V. Harish, D. N. M. Khan, R. B. Krishna, R. Singh, and S. Chaudhary, “Land slide detection and monitoring system using wireless sensor networks (wsn),” in *Proc. IEEE International Advance Computing Conference*, 2014, pp. 149–154.

[7] A. T. Aby, M. F. Servajean, *et al.*, “Impact of simulation environment in performance evaluation of protocols for WSNs,” in *Ad-hoc, Mobile, and Wireless Networks: 16th International Conference on Ad Hoc Networks and Wireless*, Messina, Italy, September 20-22, 2017, vol. 10517, p. 290.

[8] A. T. Aby, M. F. Servajean, and M. Misson, “Impact of the simulation parameters on the quantitative results of protocols for WSNs,” in *Proc. IEEE 28th Annual International Symposium on Personal, Indoor, and Mobile Radio Communications*, 2017, pp. 1–7.

[9] IEEE 802.15, “IEEE standard for local and metropolitan area networks – part 15.4: Low-rate wireless personal area networks (LR-WPANs),” ANSI/IEEE, Standard 802.15.4 R2011, 2011.

[10] A. T. Aby, A. Guitton, P. Lafourcade, and M. Misson, “History- based MAC protocol for low duty-cycle wireless sensor networks: The Slack-MAC protocol,” in *Proc. EAI Endorsed Transactions on Mo- bile Communications and Applications*, EUDL: European Union Digital Library, 2016.

[11] “Slack-MAC: Adaptive MAC protocol for low duty-cycle wireless sensor networks,” in *Ad Hoc Networks*. Springer, 2015, pp. 69–81.

[12] A. M. Kanthe, D. Simunic, and R. Prasad, “Effects of propagation models on AODV in mobile ad-hoc networks,” *Wireless personal communications*, vol. 79, no. 1, pp. 389–403, 2014.

[13] T. Monks, C. S. Currie, B. S. Onggo, S. Robinson, M. Kunc, and S. J. Taylor, “Strengthening the reporting of empirical simulation studies: Introducing the stress guidelines,” *Journal of Simulation*, pp. 1–13, 2018.

[14] M. Alduais and N. Abdulwahab, “The performance evaluation of different logical topologies and their respective protocols for wireless sensor networks,” Ph.D. dissertation, Universiti Tun Hussein Onn Malaysia, 2015.

[15] V. Bajpai, M. Ku ̈hlewind, J. Ott, J. Scho ̈nwa ̈lder, A. Sperotto, and B. Trammell, “Challenges with reproducibility,” in *Proc. Reproducibility Workshop*. ACM, 2017, pp. 1–4.

[16] W. C. Jakes and D. C. Cox, *Microwave Mobile Communications*, Wiley-IEEE Press, 1994.

[17] T. S. Rappaport, *Wireless Communications: Principles and Practice*, Prentice hall PTR New Jersey, 2002, vol. 2.

[18] A. Neskovic, N. Neskovic, and G. Paunovic, “Modern approaches in modeling of mobile radio systems propagation environment,” *IEEE Communications Surveys & Tutorials*, vol. 3, no. 3, pp. 2–12, 2000.

[19] S. Benferhat, “Simulation des conditions de trafic intracellulaire d’un r éseau sans fil en milieu industriel par un mode`le de propagation composite,” Ph.D. dissertation, Universit é Blaise Pascal- Clermont-Ferrand II, 2009.

[20] G. Chalhoub, A. Guitton, and M. Misson, “MAC specifications for a WPAN allowing both energy saving and guaranted delay- Part A: MaCARI: A synchronized tree-based MAC protocol,” in *IFIP WSAN*, 2008.

[21] K. Nguyen, Y. Ji, and S. Yamada, “Low overhead MAC protocol for low data rate wireless sensor networks,” *International Journal of Distributed Sensor Networks*, 2013.

[22] G. Lu, B. Krishnamachari, and C. Raghavendra, “An adaptive energy-efficient and low-latency MAC for tree-based data gathering in sensor networks,” in *Proc. Wireless Communications and Mobile Computing*, September 2007, pp. 863–875.

[23] W. Z. Song, R. Huang, B. Shirazi, and R. LaHusen, “Treemac: Localized TDMA MAC protocol for real-time high-data-rate sensor networks,” *Pervasive and Mobile Computing*, vol. 5, no. 6, pp. 750–765, 2009.

[24] F. D. Cunha, I. Cunha, H. C. Wong, A. A. Loureiro, and L. B. Oliveira, “ID-MAC: An identity-based MAC protocol for wireless sensor networks,” in *Proc. IEEE Symposium on Computers and Communications*, 2013, pp. 000975–000981.

[25] Y. Sun, S. Du, O. Gurewitz, and D. B. Johnson, “DW-MAC: A low latency, energy efficient demand-wakeup MAC protocol for wireless sensor networks,” in *Proc. 9th*

ACM International Symposium on Mobile ad Hoc Networking and Computing, 2008, pp. 53–62.

[26] V. Sundararaj, S. Muthukumar, and R. Kumar, "An optimal cluster formation based energy efficient dynamic scheduling hybrid MAC protocol for heavy traffic load in wireless sensor networks," *Computers & Security*, vol. 77, pp. 277–288, 2018.

[27] L. Cheng, Y. Gu, J. Niu, T. Zhu, C. Liu, Q. Zhang, and T. Hel, "Taming collisions for delay reduction in low-duty-cycle wireless sensor networks," in *Proc. 35th Annual IEEE International Conference on IEEE INFOCOM 2016*, 2016, pp. 1–9.

[28] J. Polastre, J. Hill, and D. Culler, "Versatile low power media access for wireless sensor networks," in *ACM Sensys*, November 2004.

[29] M. Buettner, Y. Gary, V. E. Anderson, and R. Han, "X-MAC: A short preamble MAC protocol for duty-cycled wireless sensor networks," in *Proc. 4th International Conference on Embedded Networked Sensor Systems*, 2006, pp. 307–320.

[30] D. Moss and P. Levis, "BoX-MACs: Exploiting physical and link layer boundaries in low-power networking," Computer Systems Laboratory Stanford University, pp. 116–119, 2008.

[31] G. Kim and J. Ahn, "On-demand synchronous X-MAC protocol," in *Proc. Computer Science and Software Engineering*, 2016, pp. 1–6.

[32] K. Nguyen, V. Nguyen, D. Le, Y. Ji, D. A. Duong, and S. Yamada, "A receiver-initiated MAC protocol for energy harvesting sensor networks," in *Ubiquitous Information Technologies and Applications*, 2014, pp. 603–610.

[33] I. Park, H. Lee, and S. Kang, "RIX-MAC: An energy-efficient receiver-initiated wakeup MAC protocol for WSNs," *KSII Transactions on Internet & Information Systems*, vol. 8, no. 5, 2014.

[34] X. Wang, X. Zhang, G. Chen, and Q. Zhang, "Opportunistic cooperation in low duty cycle wireless sensor networks," in *Proc. IEEE International Conference on Communications*, 2010, pp. 1–5.

[35] H. Yoo, M. Shim, and D. Kim, "Dynamic duty-cycle scheduling schemes for energy-harvesting wireless sensor networks," *IEEE Communications Letters*, vol. 16, no. 2, pp. 202–204, 2012.

[36] A. T. Aby, A. Guitton, and M. Misson, "Study of blind rendez-vous in low power wireless sensor networks," in *Proc. 79th Vehicular Technology Conference* (VTC Spring), 2014, pp. 1–5.

[37] Network simulator 2. (2002). [Online]. Available: http://www.isi.edu/nsnam/ns

[38] G. Kim and J. Ahn, "On-demand synchronous X-MAC protocol," in *Proc. 13th International Joint Conference on Computer Science and Software Engineering*, 2016, pp. 1–6.

[39] S. Thomas, I. Gayathri, and A. Raj, "Joint design of dijkstra's shortest path routing and sleep-wake scheduling in wireless sensor networks," in *Proc.* International Conference on Energy, Communication, Data Analytics and Soft Computing, 2017, pp. 981–986.

[40] S. M. Ghoreyshi, A. Shahrabi, and T. Boutaleb, "An opportunistic void avoidance routing protocol for underwater sensor networks," in *Proc. IEEE 30th International Conference on Advanced Information Networking and Applications*, 2016, pp. 316–323.

[41] S. Gousalya, S. Lavanya, and M. Bhagyaveni, "Opportunistic aodv routing protocol for cognitive radio wireless sensor networks," in *Proc. International Conference on Communication and Signal Processing*, 2016, pp. 0412–0415.

[42] M. C. C. Hung, K. C. J. Lin, C. F. Chou, and C. C. Hsu, "Effort: Energy-efficient opportunistic routing technology in wireless sensor networks," *Wireless communications and Mobile Computing*, vol. 13, no. 8, pp. 760–773, 2013.

[43] X. Zhong, R. Lu, L. Li, and S. Zhang, "Etor: Energy and trust aware opportunistic routing in cognitive radio social internet of things," in *Proc. GLOBECOM 2017-2017 IEEE Global Communications Conference*, 2017, pp. 1–6.

[44] C. Hsu, M. S. Kuo, S. C. Wang, and C. F. Chou, "Joint design of asynchronous sleep-wake scheduling and opportunistic routing in wireless sensor networks," *IEEE Transactions on Computers*, vol. 63, no. 7, pp. 1840–1846, 2014.

[45] L. Cheng, J. Niu, C. Luo, L. Shu, L. Kong, Z. Zhao, and Y. Gu, "Towards minimum-delay and energy-efficient flooding in low-duty-cycle wireless sensor networks," *Computer Networks*, vol. 134, pp. 66–77, 2018.

[46] Y. Zhang and M. P. J. Fromherz, "A robust and efficient flooding- based routing for wireless sensor networks," *Journal of Interconnection Networks*, vol. 7, pp. 549–568, December 2006.

[47] S. Wu, J. Niu, L. Cheng, and W. Chou, "Energy efficient flooding under minimum delay constraint in synchronous low-duty-cycle wireless sensor networks," in *Proc. Computing, Communications and IT Applications Conference*, 2014, pp. 121–126.

[48] L. Cheng, J. Niu, Y. Gu, C. Luo, and T. He, "Achieving efficient reliable flooding in low-duty-cycle wireless sensor networks," *IEEE/ACM Transactions on Networking*, no. 6, pp. 3676–3689, 2016.

[49] S. Wu, J. Niu, W. Chou, and M. Guizani, "Delay-aware energy optimization for flooding in duty-cycled wireless sensor networks," *IEEE Transactions on Wireless Communications*, vol. 15, no. 12, pp. 8449–8462, 2016.

[50] A. T. Aby, A. Guitton, and M. Misson, "Efficient flooding-based routing protocol with random wake-up for very low duty-cycle WSNs," *Journal of Communications*, vol. 10, no. 6, pp. 385–395, 2015.

[51] T. Zhu, Z. Zhong, T. He, and Z. L. Zhang, "Achieving efficient flooding by utilizing link correlation in wireless sensor networks," *IEEE/ACM Transactions on Networking (TON)*, vol. 21, no. 1, pp. 121–134, 2013.

[52] L. Xu, G. Yang, J. Xu, L. Wang, and H. Dai, "Achieving adaptive broadcasting performance tradeoff for energy-critical sensor networks: A bottom-up approach," *Computer Networks*, vol. 136, pp. 155–170, 2018.

[53] S. Yu, X. Wu, P. Wu, D. Wu, H. Dai, and G. Chen, "CIRF: Constructive interference-based reliable flooding in

asynchronous duty-cycle wireless sensor networks," in *Proc. Wireless Communications and Networking Conference*, 2014, pp. 2734–2738.

[54] D. T. Nguyen, J. Choe, T. L. Duc, D. T. Le, V. V. Zalyubovskiy, and H. Choo, "Delay-sensitive flooding based on expected path quality in low duty-cycled wireless sensor networks," *International Journal of Distributed Sensor Networks*, vol. 12, no. 8, 2016.

[55] L. Xu, J. Cao, S. Lin, H. Dai, X. Wu, and G. Chen, "Energy-efficient broadcast scheduling with minimum latency for low-duty-cycle wireless sensor networks," in *Proc. 10th International Conference on Mobile Ad-Hoc and Sensor Systems*, 2013, pp. 163–167.

[56] L. Liping, "An energy aware multipath routing algorithm for wireless sensor networks," *International Journal of Online Engineering*, vol. 13, no. 4, pp. 45–56, 2017.

[57] J. Hao, Z. Yao, K. Huang, B. Zhang, and C. Li, "An energy-efficient routing protocol with controllable expected delay in duty-cycled wireless sensor networks," in *Proc. IEEE International Conference on* in *Communications*, 2013, pp. 6215–6219

[58] A. Khan, M. Ejaz, N. Javaid, M. Q. Azeemi, U. Qasim, and Z. A. Khan, "Eeors: Energy efficient optimal relay selection protocol for underwater wsns," in *Proc. 19th International Conference on Network-Based Information Systems*, 2016, pp. 239–245.

[59] S. Guo, L. He, Y. Gu, B. Jiang, and T. He, "Opportunistic flooding in low-duty-cycle wireless sensor networks with unreliable links," *IEEE Transactions on Computers*, vol. 63, no. 11, pp. 2787–2802, 2014.

[60] Y. Zhu, J. Mei, D. Zhao, and Q. Fang, "A rendezvous mechanism for energy balance and link quality in WSNs," *Wuhan University Journal of Natural Sciences*, vol. 23, no. 2, pp. 103–110, 2018.

[61] K. Han, J. Luo, L. Xiang, M. Xiao, and L. Huang, "Achieving energy efficiency and reliability for data dissemination in duty-ycled WSNs," *IEEE/ACM Transactions on Networking*, vol. 23, no. 4, pp. 1041–1052, 2015.

[62] M. S. Mezghanni, N. Kandil, and N. Hakem, "Performance study of ieee 802.15. 4/4g waveforms over the mobile underground mine radio-channel," in *84th Vehicular Technology Conference*, 2016, pp. 1–6.

[63] M. K. Simon and M. Alouini, "Outage performance of multiuser communication systems," *Digital Communication over Fading Channels*, pp. 638–680, 2005.

Affoua Thérèse ABY is an assistant professor at ESIEE-Amiens (Engineering School of Amiens), France. She is doing her research at MIS-UPJV laboratory. She received her PhD in 2016 at Clermont-Auvergne University of Clermont-Ferrand and her MSc in 2012 at Lorraine University of Nancy, in the field of computer networks. She works at ESIEE-Amiens Engineering School as an assistant professor since september 2017. Her research interests include wireless communications, sensor networks, IoT (smart building), performance evaluation, energy-efficient MAC and Routing protocols.

Stéphane Pomportes is an assistant professor at ESIEE-Amiens (Engineering School of Amiens), France. He is doing his research at MIS-UPJV laboratory. He received his PhD in 2011 at University of Paris Sud XI, ORSAY and his Engineering degree in 2008 at ESIEE-Amiens, in the field of computer networks. He works at ESIEE-Amiens Engineering School as an assistant professor since september 2012. His research interests include wireless communications, Adhoc networks, Self-stabilizing algorithm, Interference resolution in resource allocation, IoT (smart building).

Marie-Françoise Servajean obtained her PhD thesis in Computer Science in 1990 at Université Blaise Pascal, Clermont-Ferrand in France (Artificial Intelligence and expert systems field). In 1991, she became a lecturer, teaching programming, information systems analysis and databases in the Computer Science Department of the institute of Technology in Clermont-Ferrand. She is a member of the research team "Réseaux de Capteurs Sans Fil" of the laboratory LIMOS (Clermont-Ferrand). Her current research interests are Topology switching, Smart antenna, Wireless Local Area Networks, Low Power Wireless Personal Networks, Wireless Sensor Networks, real-time systems and protocol engineering.

Michel Misson obtained his PhD thesis in nuclear physics and his "Habilitation à Diriger des Recherches" (HDR) degree in Computer Science respectively in 1979 and 2001 both at Université Blaise Pascal, Clermont-Ferrand in France. In 1983, he became a lecturer, teaching networks and system architecture in the Computer Science Department of the Institute of Technology (I.U.T.) in Clermont-Ferrand. He is now Full Professor in the Networks and Telecommunications Department, he manages the research team "Réseaux et Protocoles" and he is assistant director of the Computer Science Laboratory LIMOS-CNRS of Université Clermont Auvergne UCA. He is also deputy dean of the IUT. He served on many conference committees and journals reviewing processes. His current research interests are Wireless Local Area Networks, Low Power Wireless Personal Networks, Wireless Sensor Networks, Linear Networks, real-time systems and protocol engineering. His main topics of interest are: MAC layer and Topology switching for Wireless Sensor Networks.